where ψ' is the dimensionless skin friction, k = 0.4 and d_{50} the median bed material size. In contrast to the previous model descriptions of meandering that use extensive formulations of flow hydraulics (Johanssen & Parker, 1989; Sun *et al.,* 1996), the model applied here uses a combination of process-physics and rules (e.g. equation 2) because it is designed to operate at geologic time scales. It reproduces observed features of meandering, even those not reproduced by the more physically-realistic models, such as the formation of compound bends. Segments of the meander that move into adjacent positions create neck cutoffs as a result of the developed slope advantage. The effect of chute cuttoffs is not simulated.

A more drastic form of channel relocation, avulsion, is also simulated by the model (Figure 6). Avulsions occur when the channel aggrades above the surrounding floodplain and it becomes increasingly advantageous for the channel to choose the high sloping route downwards into floodplain, especially during bank full stages. However, channel relocation by avulsion in the model is not always triggered by this 'super elevation' process (Mackey & Bridge, 1995), but was frequently caused by errors in the dynamic remeshing algorithm. This problem was not anticipated while drafting the original project proposal, and unfortunately up to two months of time was dedicated solving the responsible bugs in the remeshing algorithm.
Besides active channel meandering, CHILD simulates another process characteristic for a fluvial system; floodplain deposition. The modelling method applied for floodplain deposition is geometrical and based on the observation that floodplain sedimentation rate decreases exponentially with distance from the main channel (Howard, 1992; 1996; Mackey & Bridge, 1995).

$$dH_{overbank} = \mu (W - z) e^{\left(-d/\lambda_{ob}\right)} \Delta t \qquad (11)$$

where $dH_{overbank}$ is the local vertical deposition increment on a floodplain node, the deposition rate constant, $_{ob}$ is the distance-decay constant at which overbank sedimentation rate decreases to zero, and d is the distance between the active floodplain node and the nearest meander channel node. The floodplain model does take into the local topography by incorporating the difference between and maximum floodwater height W and the local floodplain elevation z. The maximum floodheight

W and the duration flood events, Δt, is driven by a series of storms, which are drawn at random from a frequency distribution with user-specified mean values. (Figure 4b).

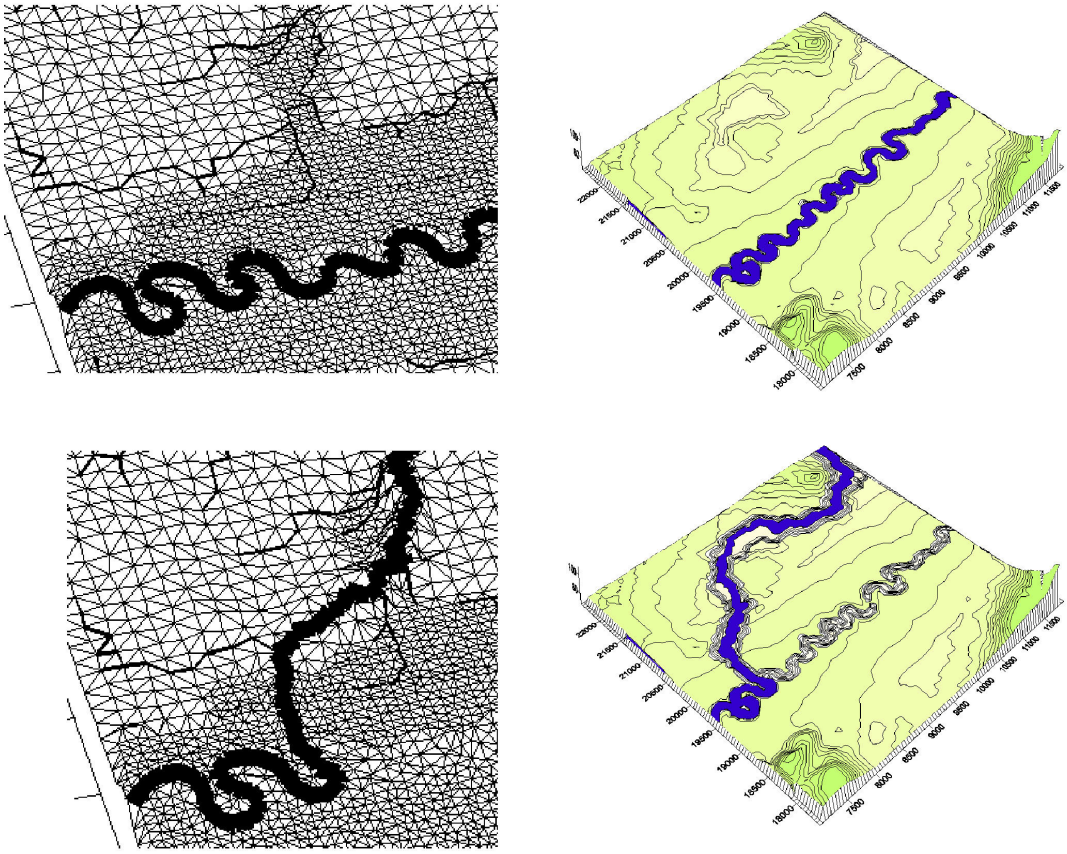

Figure 6. Example of channel relocation by avulsion. Normally, avulsions occur when the main channel aggrades above the surrounding floodplain and the channel chooses the route of maximum slope during a bank full discharge stage. However, in the model many of the avulsions were not triggered by this super elevation criterium but by errors in the remeshing algorithm. Solving these unanticipated errors turned out to consume up to two months of the project time.

For the purpose of modelling the subsurface and analyses of the preservation potential of the fluvial deposits, a subsurface stratigraphy module was added to the meander model, recording the spatial distribution of texture and ages of the fluvial sediments. For simplicity only two grainsize fractions are recorded in the stratigraphy during the meander simulations, sand deposited by the main channel and fines distributed by the overbank deposition routine (equation 11).

In an earlier version of the model the stratigraphy was connected to the triangular irregular mesh. This data structure required repeated interpolation of stratigraphic stacks during relocation and addition of meander nodes in order to update the stratigraphy at new node positions. As a result of frequent node movement over the

mesh and the subsequent interpolation, the stratigraphic information was partially lost. The new statigraphic routine created in this study uses an auxiliary, static mesh to store the layer stacks and is of higher stratigraphic resolution (0.015-0.05 m).

4. Visualisation results

4.1 Visualisation of floodplain landscape evolution and subsurface stratigraphy

An example of a modelled floodplain landscape is shown in figure 7, where the evolution of the meander channel is given in time steps 1500 yrs. The system starts of as an initially straight channel superposed upon a digital terrain model of a floodplain. Minor irregularities in the channel pattern at 500 yrs evolve to a set of complete bends at the verge of straightening by cut-offs at T = 3500 yrs. Around T=5000 - 6500 yrs the outlines of the main channel belt are delineated by the first abandoned meander loops. The contour lines within these loops and those flanking the active channel reflect the ages of the sediment deposited by the moving channel and are spaced 300 yrs. The density of the contourlines is not uniform therefore record the differential rates of bend migration within the channel belt. The sediments within channel belt are partly reworked by growth of new bends and the complete pattern becomes more and more complex. The surrounding floodplain is gradually buried by overbank deposition and forms a slightly convex topography at the end of the simulation (Figure 8). In order to visualize the subsurface architecture of this meander-floodplain landscape at T=15000, a set of stratigraphic cross-sections were made (Figure 9). The positions of the section lines are indicated on figure 8.

The cross-sections are composed of voxels of which the intensity of red corresponds to the fraction gravel in the layers (figure 9). Paleo-channel positions are indicated by red voxels, whereas the floodplain fines are represented by blue voxels. Timelines in the cross-sections (white) are spaced 500 yrs, and show the rapid aggradation throughout this simulation (1.0 m/kyr). Minor incision is recognisable close to the channel voxels and reflects the channel depth. The section parallel to the direction of flow reveals ‘U-shaped’ structures, which develop when a meander loop migrates through the line of section. Initially, a loop is visible as a point at the moment it enters the line of section. As the loop grows and migrates through the section line, the upstream and down stream branch are recorded.

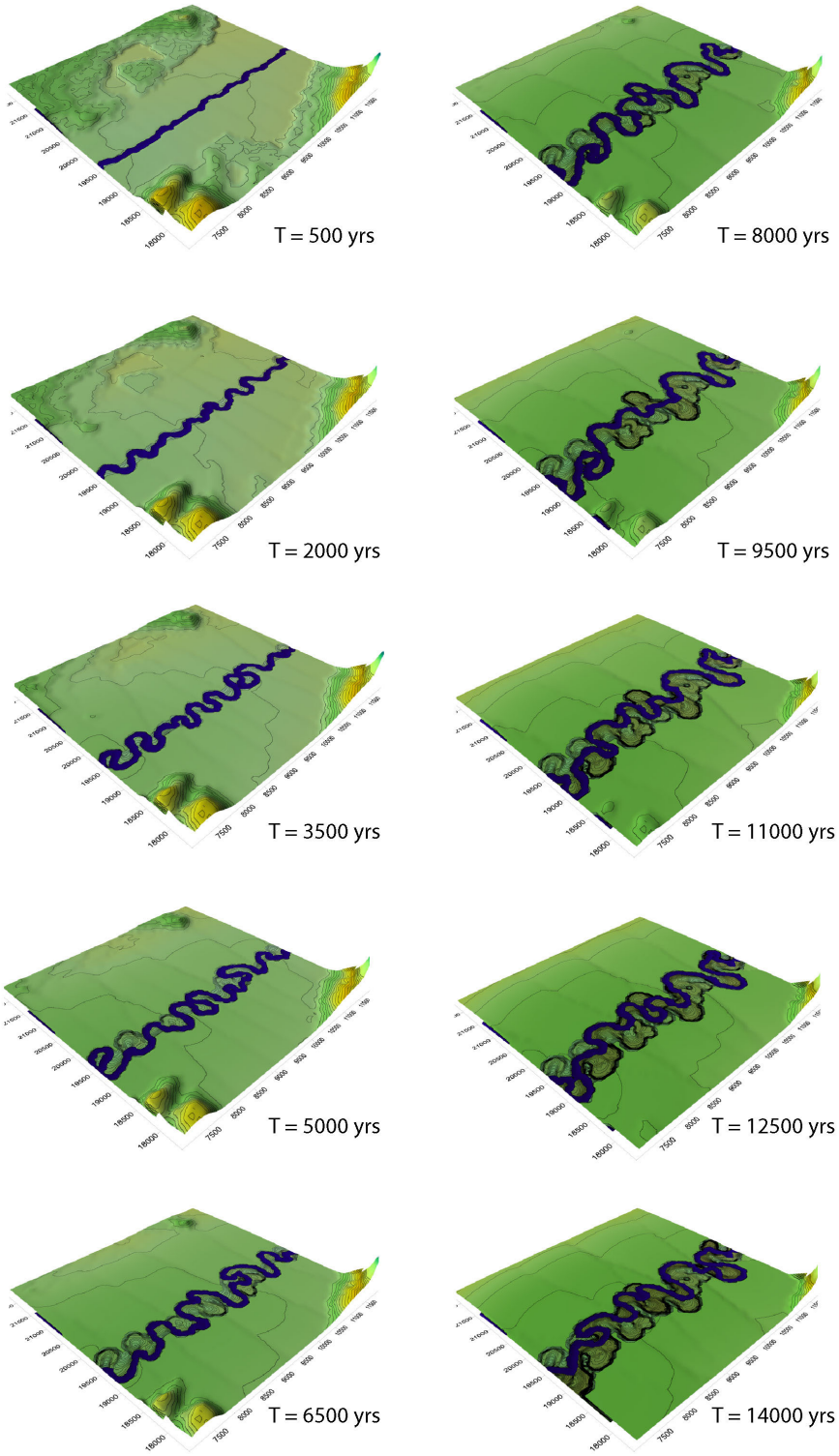

Figure 7. Landscape snapshots illustrating the development of the meander pattern through time. Contours in the active channel belt indicate the ages in the top layer of the stratigraphy. Contour lines are spaced 300 yrs. Note that the relief in the surrounding area is gradually buried by floodplain deposition.

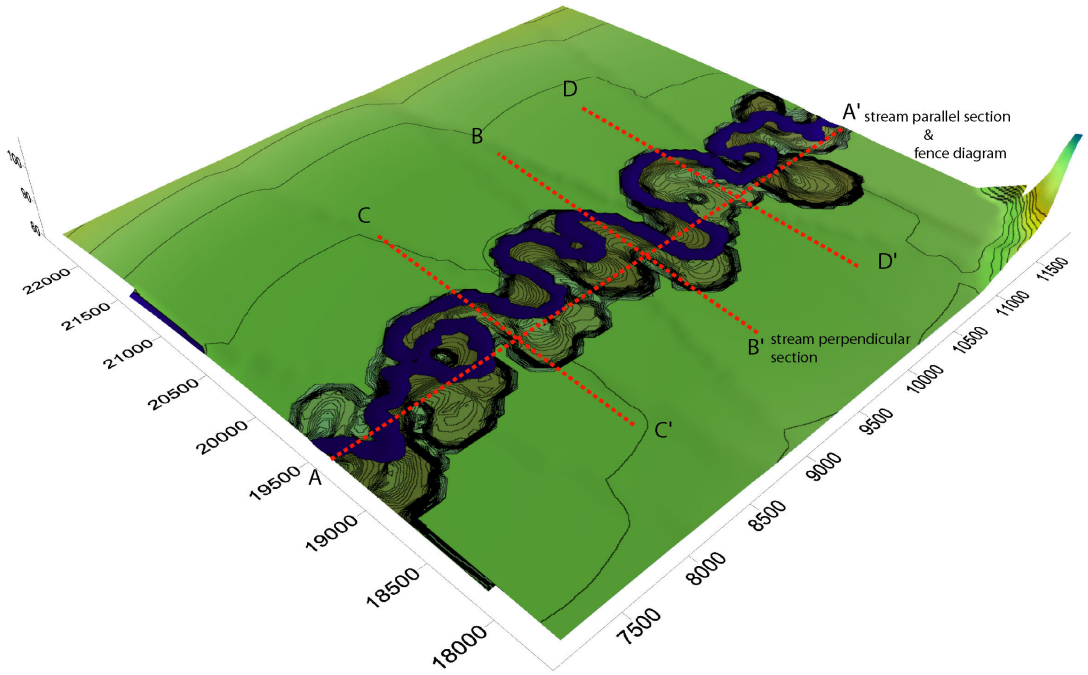

Figure 8. Meander-floodplain system belonging to the evolutionary sequence shown in figure 7, at T= 15000 yrs). Contour lines surrounding the active channel reflect the ages of the sediment in the top layer of the stratigraphy, and are spaced 300 yrs.

Finally, both branches are abandoned abruptly due to an upstream cut-off and floodplain fines cover the paleo-channel positions. The U-shaped paleo-channels are deflected to the right, reflecting the downstream migration of the meander bends (Figure 9a & c). In stream perpendicular section the stratigraphic pattern is simpler (Figure 9b). Here the section is marked by a gradually shifting paleo-channel position, followed by abrupt channel relocation in the centre of the figure. This is the result of an upstream cut-off, not an avulsion.

Another way of illustrating the subsurface structure of the model floodplain is by visualizing a selection of voxels. In figure 10 all voxels with a gravel fraction of 0.9 and larger are shown with respect to the floodplain surface and the position of the river at the end of the simulation at T=15000. Clearly, these voxels are not uniformly interconnected and their distribution widens upwards towards the surface, a pattern that is indicative of the widening of the channel belt. Statistical analysis of voxel volume and connectivity, generated by a suite of simulations, could be used to for groundwater flow simulations and to aid predictions in gravel exploration.

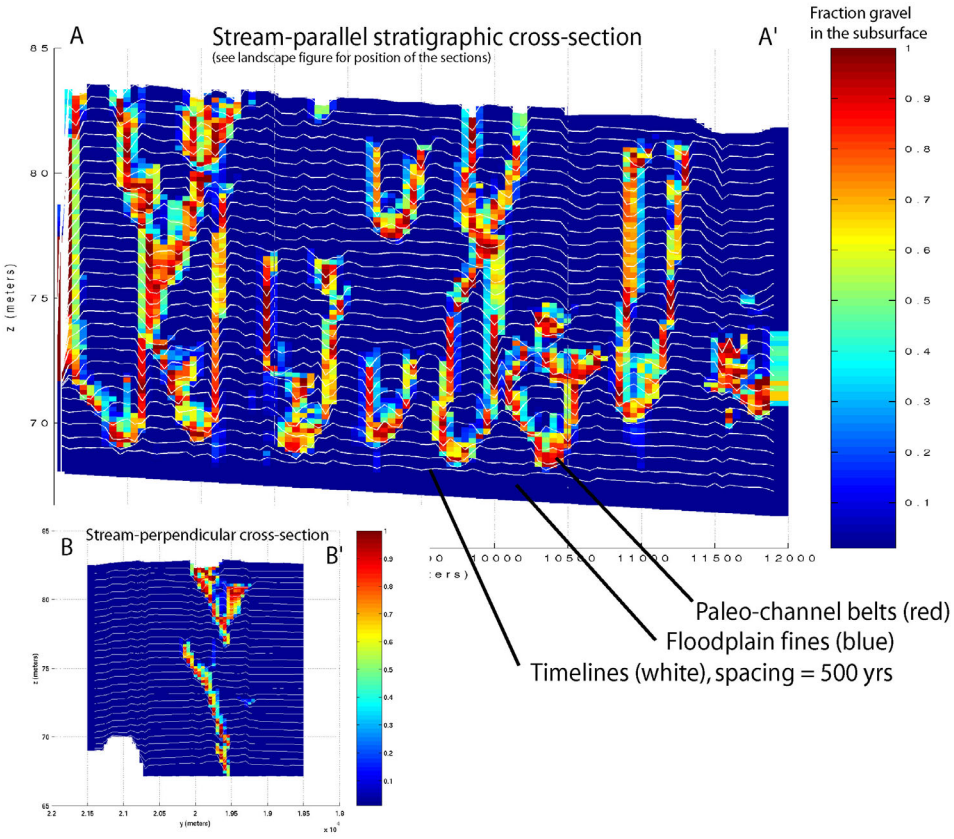

Figure 9a & b. Stratigraphic cross-sections through this system show the subsurface distribution of paleo-channels (red, sand) and floodplain fines (blue, clays). Timelines in the cross-sections (white) are spaced 500 yrs, and show the rapid aggradation throughout this simulation (1.0 m/kyr). The stream parallel sections are dominated by U-shaped configurations of paleo channels, indicating the growth of bends through the line of section. The stream perpendicular section shows the sideways shift of the channel positions due to growth of loops.

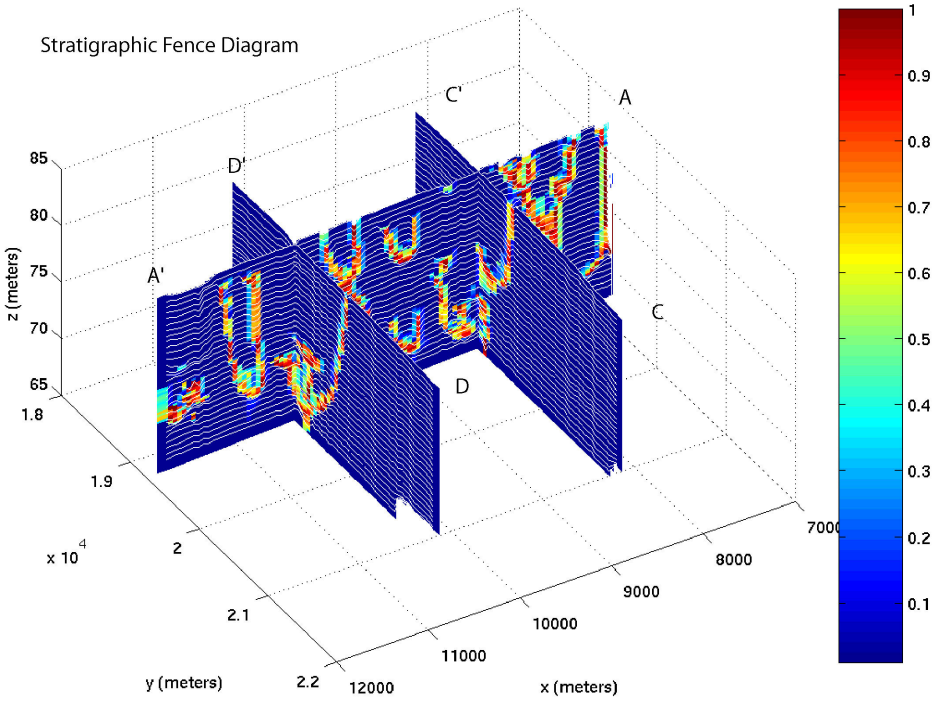

Figure 9c. Fence-diagram showing the subsurface stratigraphy of the modelled floodplain-meander landscape. Red colours represent paleo channels, blue floodplain fines and the white timelines are spaced 500 yrs. Capital letters correspond to position of the sections in the landscape figure 8.

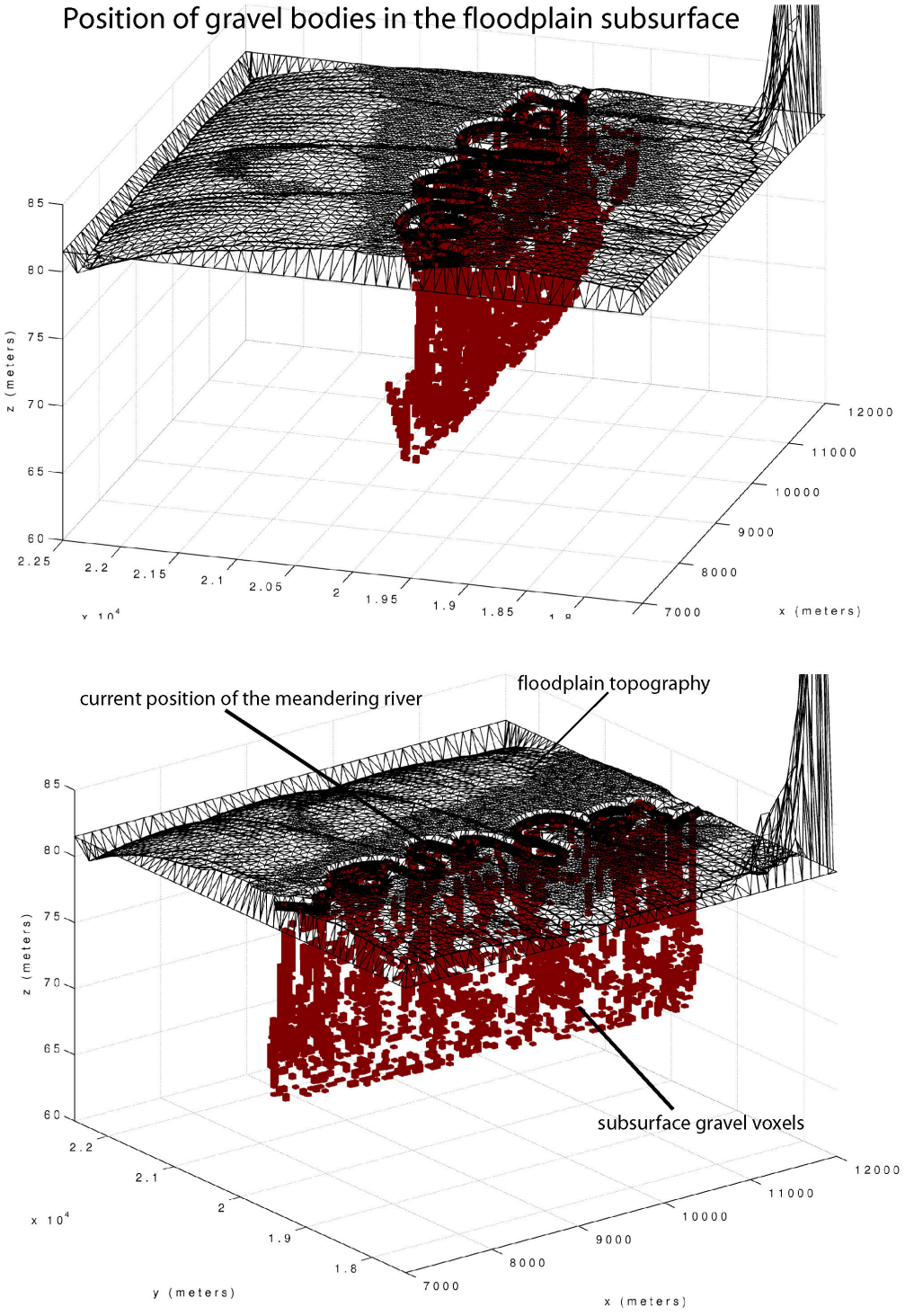

Figure 10. Block diagrams showing the distribution of paleo-channel voxels with a sand fraction larger than 0.9 in the subsurface of the modelled floodplain.

5. Model runs set 1, sensitivity analysis

5.1 Sensitivity to key variables

A set of experiments is conducted to study the sensitivity of the river sinuosity to key variables in the model; the channel bed aggradation rate (Fig. 11a), the bank erodability (Fig. 11b) and the storm intensity (Fig. 11c). All curves in figure 11 show a steep increase of sinuosity for the first 4000-6000 yrs followed by a sawtooth pattern of sinuosity fluctuating around a mean of 2 to 3. This sawtooth pattern of gradual increase followed by a sudden fall in sinuosity, reflects the growth and straightening of bends within the meander belt. For low storm intensities this pattern has a clear periodicity of 1500 yrs (P_{mean} = 15m/yr, Fig. 11c). Furthermore, increasing the storm intensity, bankerodability and aggradation rate result in irregular fluctuations in sinuosity. This corresponds to a more complex channel pattern dominated by compound loops and stepped growth and straightening of bends and therefore superposed periodicities.

5.2 Sensitivity to perturbation

In the following two experiments (Figure 12) the meander system was run through an initial 5000 yrs start-up phase and the subjected to a short, 2000 yrs perturbation in the form of increased aggradation rate or storm intensity. The effects on the development of channel sinuosity and channel belt width are compared to a system that was not perturbed (e.g. control run) in figures 12A and 12B. Both temporal increases in channel bed aggradation rate and storm intensity result in a divergence of the sinuosity trends in the 1000 yrs after the perturbation. Only in the experiment with the raised storm intensity the sinuosity is already affected during the perturbation.

The effect of storm intensity is evident in figure 12B, in which the growth of channel width accelerates during the perturbation phase but also in the 2000 yrs afterwards. As a result of this acceleration, the occurrence of cut-off events is earlier and their effect is amplified.

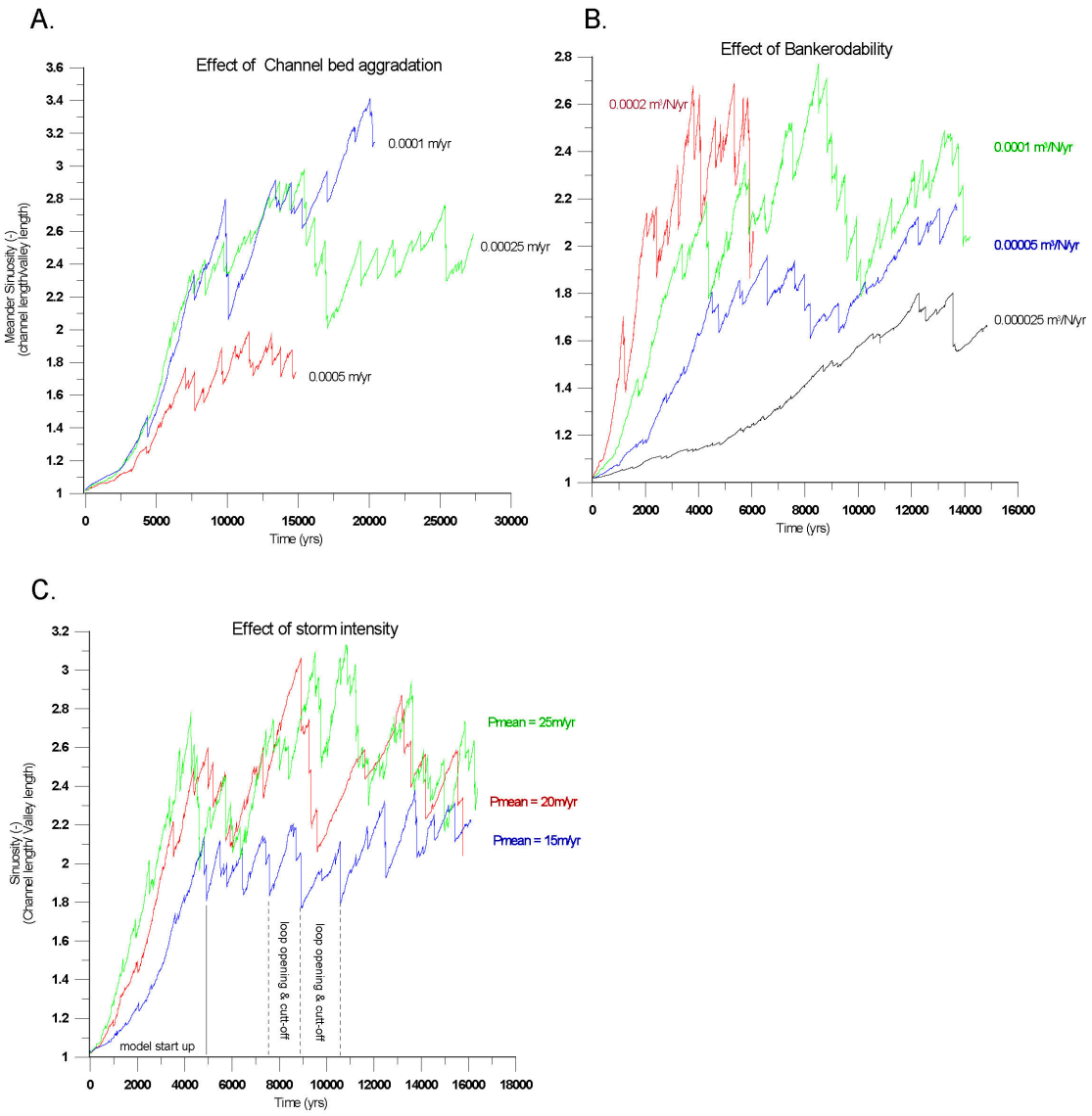

Figure 11. Effect of (a) channel bed aggradation rate, (b) Bank erodability and (c) mean storm intensity on the 'sinuosity' of the modelled meander. The average time scale for the model to reach a 'dynamic equilibrium' is 5000 yrs, but this is highly dependent on the value of the bank erodability. The saw-tooth pattern visible in all graphs reflects the gradual growing of meander loops followed by the development of cut-offs. For lower storm intensities this pattern has a clear periodicity of ~ 1500 yrs. Increasing storm intensity, bank erodability results in larger composite meander loops and more complex, superposed cut-off 'periodicities'.

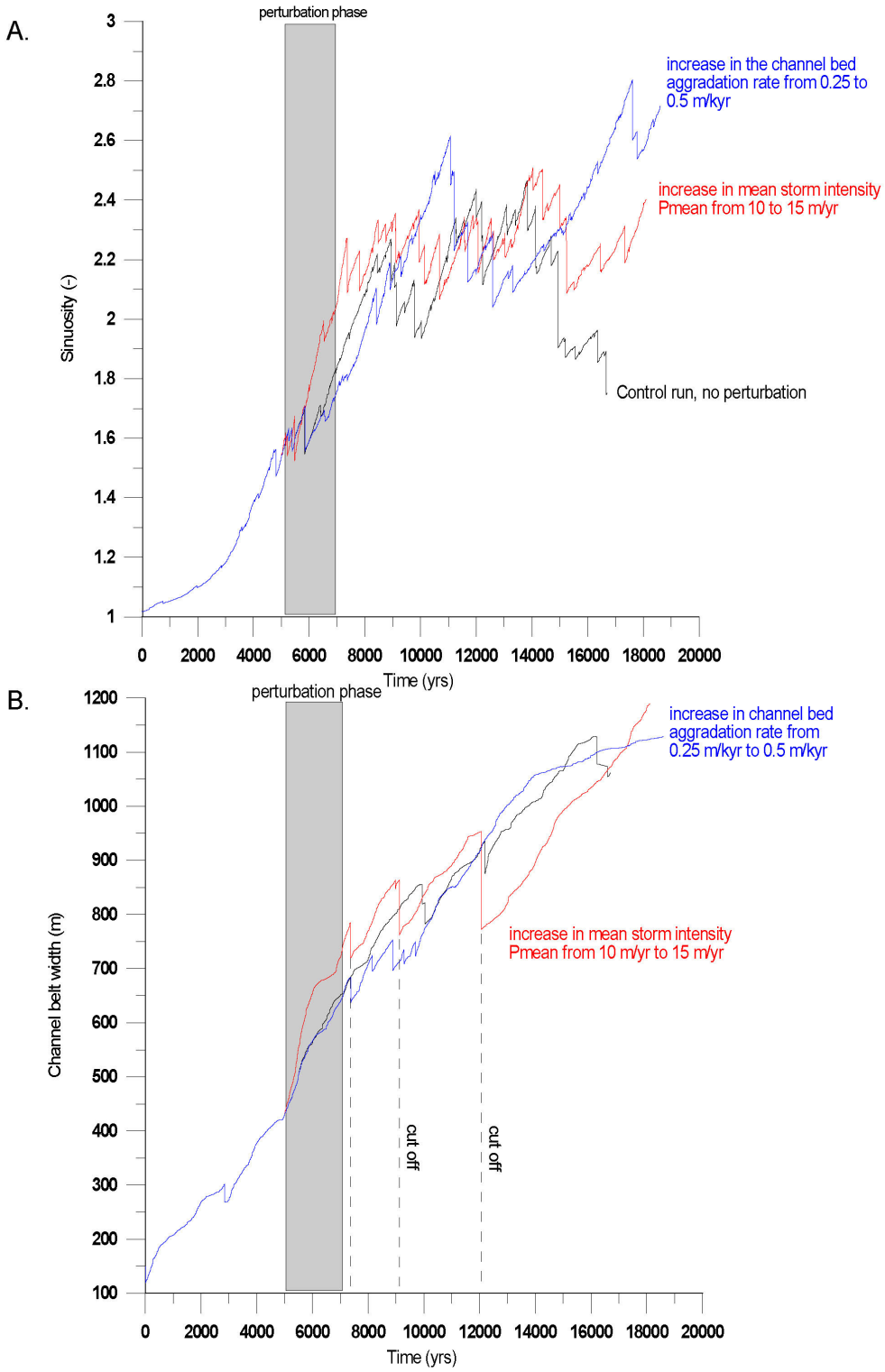

Figure 12. The effects of a 2000 yr long increase in channel bed aggradation rate (blue) and storm intensity (red) on the meander sinuosity and channel belt width trends. The effect of the storm pulse is that it amplifies the growth rate of the channel belt and cut-off magnitude long after the pulse has ceased (7000-12000 yr, fig. B). This has implications for the alluvial unit preservation potential, Figure 13.

5.3 The effect of perturbation on the preservation potential of the stratigraphy

The preservation potential of alluvial sediments is also affected by the perturbations in channel aggradation rate and storm intensity. Figure 13A shows the volume of sediment present the subsurface at T = 18000 yrs as a function of its age. Sediment ages are defined by grouping the sediments into fluvial packages with a lifetime of 300 yrs.

As result of channel bed aggradation rate the volume of sediment increases rapidly during the perturbation, but also in the subsequent 1000-1500 yrs. This increase in deposited volume reflects the delayed infilling of the floodplain topography as overbank deposition tries to catch op with the previous phase of rise of the channel.

The storm intensity perturbation results in an increased in deposited volume, but also effects the preservation of units that are younger than the perturbation. Units with an average age of 7800, 9500 and 11500 yrs, are less well preserved in the subsurface at time = 18000 yrs. Their ages correspond with the post-perturbation acceleration of channel width increase (compare Figs. 12B and 13A). In order to verify that this effect reflects variability in preservation and not original deposition volume the preservation is also expressed as a ratio (Fig. 13B). This ratio is defined as the volume of a fluvial unit at T =18000, divided by the original deposited volume. Again, a reduction in preservation is indicated for the younger fluvial units deposited in the 2000 yrs after the perturbation. The error in this particular graph is approx. 5% due to resolution of the stratigraphy. In the following experiments the resolution is increased and the error limited to less than 1%.